

Single [101]-oriented growth of $\text{La}_{0.9}\text{Sr}_{0.1}\text{MnO}_3$ films on vicinal $\text{SrTiO}_3(001)$ substrates

M. J. Zhuo, Y. L. Zhu, and X. L. Ma^{a)}

Shenyang National Laboratory for Materials Science, Institute of Metal Research,
Chinese Academy of Sciences, 110016 Shenyang, People's Republic of China

H. B. Lu

Laboratory of Optical Physics, Institute of Physics, Chinese Academy of Sciences, 100080 Beijing,
People's Republic of China

(Received 31 October 2005; accepted 11 January 2006; published online 13 February 2006)

Thin films of orthorhombic $\text{La}_{0.9}\text{Sr}_{0.1}\text{MnO}_3$, have been grown by computer-controlled laser molecular-beam epitaxy on $\text{SrTiO}_3(001)$ substrate and vicinal $\text{SrTiO}_3(001)$ substrates. Electron diffractions and high-resolution imaging reveal that the as-received thin films with thickness of 300 nm are epitaxially grown on the substrates. The microstructures in the film grown on $\text{SrTiO}_3(001)$ substrate are clarified in terms of the oriented microdomains, while the films on vicinal $\text{SrTiO}_3(001)$ substrates are predominated by a single [101]-oriented growth, which provides a useful routine for a design of preferred physical properties. Based on the minimization of surface energy, the mechanism of such a single domain formation is proposed. © 2006 American Institute of Physics. [DOI: 10.1063/1.2172141]

Ever since the discovery of colossal magnetoresistance in perovskite-type $\text{La}_{1-x}\text{A}_x\text{MnO}_3$,¹⁻⁴ interest in the microstructures of these materials associated with magnetic, electrical, and optical properties has grown considerably for understanding the mechanisms underlying their behaviors. Although thin films of these oxides have been prepared in the past few years, the microstructural characteristics in these films are unavoidably domain oriented rather than single crystalline,⁵⁻⁸ no matter whether the films are thin or thick. It has been reported that some properties of the thin films, such as magnetoresistance (MR), are sensitive to the domain orientation. For example, Amaral *et al.*⁹ found that the transport properties of MR and electrical resistivity show crystalline anisotropy in epitaxial $\text{La}_{2/3}\text{Ca}_{1/3}\text{MnO}_3$ thin films with different growth orientations. Thus, the growth of a film with single domain or with specific crystallographic orientation on a foreign substrate is needed in order to better control the properties.

Vicinal substrates have been used to grow various high crystalline quality thin films, such as $\text{YBa}_2\text{Cu}_3\text{O}_7$,^{10,11} $\text{Sr}_{1-x}\text{Ca}_x\text{RuO}_3$,¹² and $(\text{La},\text{Sr})_2\text{CuO}_4$.¹³ It is generally believed that the step flow growth of thin films on the vicinal substrate induces the formation of preferential domains and enhances their properties.^{14,15} In this letter, we report the preferred oriented growth of orthorhombic $\text{La}_{0.9}\text{Sr}_{0.1}\text{MnO}_3$ films grown on vicinal $\text{SrTiO}_3(001)$ substrates and propose the mechanism of such a single domain formation.

$\text{La}_{0.9}\text{Sr}_{0.1}\text{MnO}_3$ (LSMO) films with a thickness about 300 nm were grown on SrTiO_3 (STO)(001) substrate with miscut angles of 10° and 30° towards [100] direction of STO crystal by laser molecular beam epitaxy. For comparison, we also deposited LSMO films on exact STO(001) substrate. Detailed deposition procedure can be found in our previous article.¹⁶ A JEOL 2010 transmission electron microscope (TEM) with a point resolution of 0.194 nm was used for the

electron diffraction analysis and atomic imaging.

STO has a perfect cubic perovskite structure with a lattice parameter of $a=0.3905$ nm. LSMO has a distorted perovskite structure which exhibits an orthorhombic variant. Its lattice parameters in its bulk form at room temperature are: $a=0.55469$ nm, $b=0.77362$ nm, and $c=0.556033$ nm.¹⁷ It is theoretically proposed that when the LSMO film epitaxially grows on the STO(001), there are six possible growth orientations, or to say, the film has six orthorhombic variants or domains.¹⁸ Since the lattice parameters of a_o and c_o are approximately the same and therefore $[101]_o$ direction is not, but rather closely, perpendicular to the $[10\bar{1}]_o$, electron diffraction may only make three of these domains distinguishable.

Figure 1(a) is a low-magnification cross-sectional image of LSMO films on exact (001)STO, showing a sharp, flat and well-defined LSMO/STO interface and a columnar structure. The columnar structure in the film likely originates from the interface between the film and substrate. The corresponding selected area electron diffraction (SAED) pattern is shown in Fig. 1(b). The existence of three types of super-diffraction spots indicates the three-domain structure of the film.⁷ Figure 1(c) is a plan-view image showing the oriented domains form a rectangular cross-grid pattern. Such a configuration is believed to balance the lattice mismatch between variant domains and the STO substrate.

In contrast, the LSMO films grown on vicinal STO(001) substrate exhibit more uniform structure. Figure 2(a) shows a low-magnification cross-sectional image of the film on 10° miscut (001)STO substrate, in which neither domains nor intermediate layers were observed. The films on 30° miscut vicinal substrates exhibit similar microstructural characteristics to that of the 10° miscut one. Figure 2(b) is a SAED pattern corresponding to the area in Fig. 2(a), which is indexed as a single $[010]_o$ zone axis of the orthorhombic LSMO variant. Figure 2(c) is a plan-view image showing an overview of microstructures in the film, which confirms no distinct domains as that in Fig. 1(c). The SAED pattern cor-

^{a)} Author to whom correspondence should be addressed; electronic mail: xlma@imr.ac.cn

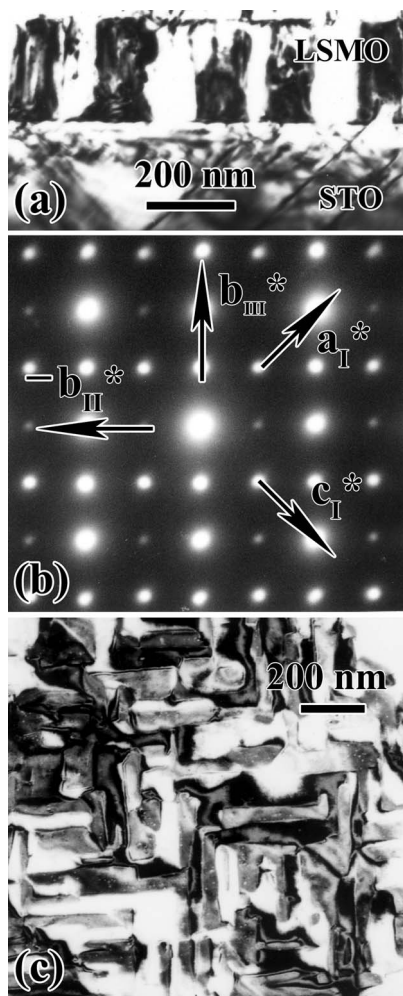


FIG. 1. (a) A low-magnification cross-sectional image of LSMO films on exact (001)STO. (b) Composite electron diffraction patterns of three oriented domains corresponding to Fig. 1(a). (c) A plan-view image showing the oriented domains form a rectangular cross-grid pattern.

responding to Fig. 2(c) is shown in Fig. 2(d), which is indexed as a single $[101]_o$ zone axis of the orthorhombic LSMO variant. Such an electron diffraction analysis indi-

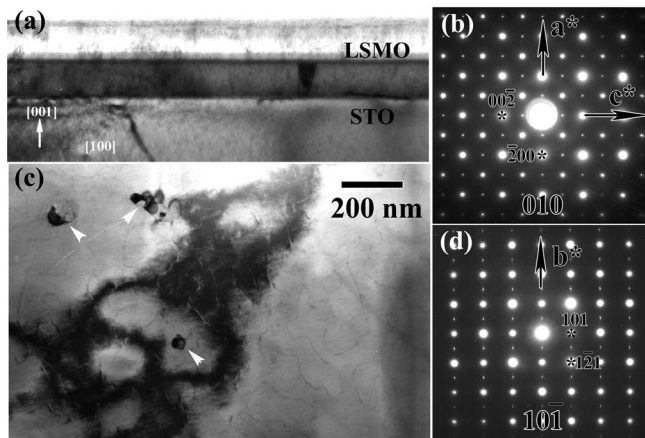


FIG. 2. (a) A low-magnification cross-section image of the film on 10° miscut (001)STO substrate. (b) Electron diffraction pattern of (a), which is indexed as a single $[010]_o$ zone axis of the orthorhombic LSMO variant. (c) Plan-view image showing an overview of microstructures in the film, and no distinct domains as that in Fig. 1(c) is observed. (d) Electron diffraction pattern taken from plan-view specimen, indicating that the film is single $[101]_o$ -oriented growth rather than multi-domain intergrowth.

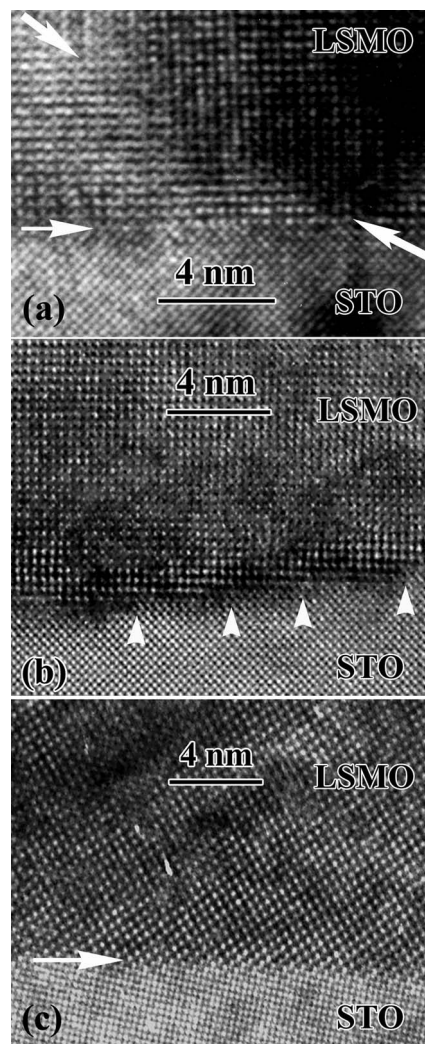


FIG. 3. Cross-sectional high-resolution images showing the interface between the LSMO film and STO substrate. (a) The film is grown on exact (001) STO, two oriented domains are seen in the image and their boundary is marked with two thick white arrowheads; (b) on 10° miscut STO, atomic steps at the interface are indicated by white arrowheads; (c) on 30° miscut STO. It is seen that all these films are epitaxially grown on the substrate, and films on vicinal substrate are single domain oriented.

cates that the film is single $[101]_o$ -oriented growth rather than multi-domain intergrowth.

Figures 3(a)–3(c) show the cross-section high resolution images taken with the incident beam parallel to the $[010]_c$ direction; showing atomic scale information on the epitaxial growth across the LSMO/STO interface of different films. Figure 3(a) shows an atomically sharp interface of the film on exact (001)STO. Two oriented domains are seen in the image and their boundary is marked with two thick white arrowheads. Figures 3(b) and 3(c) are high-resolution electron microscope (HREM) images of the films grown on vicinal substrate, 10° and 30° miscut, respectively. Atomic steps at the interface in Fig. 3(b) are marked with white arrowheads; it is seen that such steps do not have the same height and length.

Based on the above SAED and HREM experiments, it was found that the film grown on exact (001)STO consists of several oriented domains, while the films on vicinal substrates are predominated with $[010]_o$ -oriented growth. Such a microstructural difference indicates that the substrate surface has a nonductile effect on the domain structure of the

epitaxial films. The misfits between an orthorhombic LSMO and cubic STO substrate along the $[100]_c$, $[010]_c$, and $[001]_c$ directions are 0.945% or -0.95% . From the viewpoint of lattice misfit, different domains would grow alternatively to compensate the compressive or tensile strain in spite of the morphology of the substrates. However, only single oriented domain is favored in the films on vicinal substrates in the present study. In other words, the minimization of lattice mismatch failed to determine the single-domain film growth.

Generally, the minimization of lattice mismatch (strain energy) is taken into account in the explanation of the thin film crystallographic structure deposited on different substrates.^{19,20} In fact, the role of surface energy is also relevant in discussing this film growth issues. Ricci *et al.*²¹ addressed the mechanism of domain selection in terms of free energy minimization, including both strain and surface energy contribution. They revealed that the minimization of surface energy plays an important role in determining the film growth orientation as the CaRuO_3 thin film on $\text{LaAlO}_3(110)$ substrate. In the $\text{YBa}_2\text{Cu}_3\text{O}_7$ system, some researchers have shown that the anisotropy of surface energy, rather than minimization of strain, is fundamental both in determining the unit cell orientation and the relative orientation of a - b axes.^{22,23}

The surface energy (U) minimization is applied to solve the problem of the orientation of the domain in our work. The fact that the $\{101\}_o$ planes have higher surface energy than $(010)_o$ plane can be understood based on the relatively crude argument according to Ref. 22. Roughly, we imagine that the surface energy is related to the dangling bonds that are obtained when a surface is created by breaking apart a crystal along a given crystallographic plane. Meanwhile, we neglect the variation of bond energies due to the different atomic rearrangements and suppose that the orthorhombic structure is the evolution of a cubic structure, then the same kind of dangling bonds are obtained along cuts parallel to (100) or to (010) or to (001) facets of the cubic. The ratio of surface energies (U) grossly corresponds to the ratio of bond densities (D). During the cubic to orthorhombic transition, the number of bonds (N) remains constant in the $\{101\}_o$ and $(010)_o$ facets which are the counterparts of the $\{001\}$ facets in cubic structure, but the area (S) of $\{101\}_o$ facets (about 0.609 nm^2) is smaller than $(010)_o$ facets (approximately 0.6216 nm^2). Therefore, through simple calculation with the formula

$$D = N/S, \quad (1)$$

higher bond density belonging to $\{101\}_o$ facet was obtained. In other words, the $\{101\}_o$ facet has higher surface energy. When there is a miscut on the substrate surface, the fourfold symmetry of (001) is broken by exposing the (100) planes at the surface steps. In order to minimize the surface energy, the relationships of $(10\bar{1})[010]_o // (001)[010]_c$ in the present study would be preferred.

In the present film on exact $(001)\text{STO}$, the formation of oriented domains is believed to result from the strain relaxation. On the other hand, as to the films on the vicinal substrates, though the formation of preferred domain can be explained by the minimized surface energy, very high strain energy should remain in the films. Such a kind of strain is relaxed through the formation of a few island-like nanoparticles embedded in the films as marked with white arrows in

Fig. 2(c). Nanobeam analysis shows that such nanoparticles have a similar chemical composition and lattice constants with their surrounding medium, as a result, the strain can be effectively relieved. Simultaneously the relaxation of the strain further contributes to the preferred oriented growth.^{24,25}

In conclusion, the formation of oriented domains in LSMO films has been prevented via using miscut STO substrates. Instead, films with single $[101]$ -oriented growth are deposited on the vicinal $\text{STO}(001)$ substrates, which might provide a useful routine for a design of preferred physical properties. The mechanism of such a single domain growth is proposed on the basis of the minimization of surface energy on the vicinal $\text{STO}(001)$ substrates.

This work was supported by the National Outstanding Young Scientist Foundation for X.L.M. with Grant No. 50325101, National Natural Science Foundation (No. 10334070) and the Special Funds for the Major State Basic Research Projects of China (Grant No. 2002CB613503).

¹S. Jin, T. H. Tiefel, M. McCormack, R. A. Fastnacht, R. Ramesh, and L. H. Chen, *Science* **264**, 413 (1994).

²R. Von Helmolt, J. Wecker, B. Holzapfel, L. Schultz, and K. Sanwer, *Phys. Rev. Lett.* **71**, 2331 (1993).

³J. F. Mitchell, D. N. Argyriou, C. D. Potter, D. G. Hinks, J. D. Jorgensen, and S. D. Bader, *Phys. Rev. B* **54**, 6172 (1996).

⁴H. L. Ju, C. Kwon, Q. Li, R. L. Greene, and T. Venkatesan, *Appl. Phys. Lett.* **65**, 2108 (1994).

⁵O. I. Lebedev, G. Van Tendeloo, A. M. Abakumov, S. Amelinckx, B. Leibold, and H. U. Habermeier, *Philos. Mag. A* **79**, 1461 (1999).

⁶X. L. Ma, Y. L. Zhu, X. M. Meng, H. B. Lu, F. Chen, Z. H. Chen, G. Z. Yang, and Z. Zhang, *Philos. Mag. A* **82**, 1331 (2002).

⁷Y. L. Zhu, X. L. Ma, D. X. Li, H. B. Lu, Z. H. Chen, and G. Z. Yang, *Mater. Lett.* **58**, 1485 (2004).

⁸M. Zhang, X. L. Ma, D. X. Li, H. B. Lu, Z. H. Chen, and G. Z. Yang, *Phys. Status Solidi A* **196**, 365 (2003).

⁹V. S. Amaral, A. A. C. S. Lourenco, J. P. Araújo, P. B. Tavares, E. Alves, J. B. Sousa, J. M. Vieira, M. F. da Silva, and J. C. Soares, *J. Magn. Magn. Mater.* **211**, 1 (2000).

¹⁰D. H. Lowndes, X. Y. Zheng, S. Zhu, J. D. Budai, and R. J. Warmack, *Appl. Phys. Lett.* **61**, 852 (1992).

¹¹D. G. Schlom, D. Angelmetti, J. D. Bednorz, R. F. Broom, A. Catana, T. Frey, C. Gerber, H. J. Guntherodt, H. P. Lang, and J. Mannhart, *Z. Phys. B: Condens. Matter* **86**, 163 (1992).

¹²C. B. Eom, R. J. Cava, R. M. Fleming, J. M. Phillips, R. B. van Dover, J. H. Marshall, J. W. P. Hsu, J. J. Krajewski, and W. F. Peck, Jr., *Science* **258**, 1766 (1992).

¹³J. Kwo, R. M. Fleming, H. L. Kao, D. J. Werder, and C. H. Chen, *Appl. Phys. Lett.* **60**, 1905 (1992).

¹⁴M. Fatemi, A. E. Wickenden, D. D. Koleske, M. E. Twigg, J. A. Freitas, Jr., R. L. Henry, and R. J. Gorman, *Appl. Phys. Lett.* **73**, 608 (1998).

¹⁵D. Vassiloyannis, *IEEE Trans. Appl. Supercond.* **9**, 1638 (1999).

¹⁶T. Zhao, H. B. Lu, F. Chen, S. Y. Dai, G. Z. Yang, and Z. H. Chen, *J. Cryst. Growth* **212**, 451 (2000).

¹⁷D. E. Cox, T. Iglesias, E. Moshopoulou, K. Hirota, K. Takahashi, and Y. Endoh, *Phys. Rev. B* **64**, 024431 (2001).

¹⁸J. C. Jiang, W. Tian, X. Pan, Q. Gan, and C. B. Eom, *Mater. Sci. Eng., B* **56**, 152 (1998).

¹⁹C. J. Lu, Z. L. Wang, C. Kwon, and O. X. Jia, *J. Appl. Phys.* **88**, 4032 (2000).

²⁰I. Maclaren, Z. L. Wang, H. S. Wang, and Q. Li, *Philos. Mag. A* **82**, 1405 (2002).

²¹F. Ricci, M. F. Bevilacqua, F. M. Granozio, and U. S. di Uccio, *Phys. Rev. B* **65**, 155428 (2002).

²²F. M. Granozio and U. S. di Uccio, *J. Cryst. Growth* **174**, 409 (1997).

²³F. M. Granozio, M. Salluzzo, U. S. di Uccio, I. Maggio-Aprile, and Ø. Fischer, *Phys. Rev. B* **61**, 756 (2000).

²⁴Y. L. Zhu, X. L. Ma, D. X. Li, H. B. Lu, Z. H. Chen, and G. Z. Yang, *J. Mater. Res.* **20**, 571 (2005).

²⁵D. X. Huang, C. L. Chen, L. Chen, and A. J. Jacobson, *Appl. Phys. Lett.* **84**, 708 (2004).